Structural Requirements for Adhesion of Soluble Recombinant Murine Vascular Cell Adhesion Molecule-1 to $\alpha 4\beta 1$

Mark E. Renz, Henry H. Chiu, Susan Jones, Judy Fox,‡ K. Jin Kim,§ Leonard G. Presta,* and Sherman Fong

Departments of Immunology and *Protein Engineering, ‡Cell Biology and Metabolism Group, and §Hybridoma Group, Genentech, Inc., South San Francisco, California 94080

Abstract. This study describes the identification of seven amino acid residues of the vascular cell adhesion molecule (VCAM-1) that influence binding to the $\alpha 4\beta 1$ receptor. Using recombinant murine VCAM-1-IgG, which is bound by both mouse (WEHI 231) and human (Ramos) lymphoid cells, two approaches demonstrated the crucial role of the first two NH_2-terminal Ig-like domains in binding: (*a*) blocking monoclonal anti-mouse VCAM-1 antibodies bound to only truncation variants that included the first two domains; (*b*) site-direct mutagenesis of the first NH_2-terminal domain showed that alanine substitution of the amino acid residues R36, D40, K46, S54, N65, T72, and E81 partially or completely reduced adherence by human and/or mouse cells. Of these D40, when mutated to A, N, or K (but not E), showed complete abrogation of adherence by mouse and human cells, as well as inability to bind blocking anti-murine VCAM-1 antibody MVCAM.A429, while not inducing gross structural perturbations in VCAM-1. By molecular modeling, the D40 residue was located on a β turn connecting two β strands defined as C and D. The residues R36, K46, S54, N65, T72, and E81, which perturb cell adherence and caused small changes to gross structure, are conformationally near or adjacent to D40. Although these residues, identified as crucial for cell adhesion, are all located in domain 1, it is evident that there is a structural requirement for domains 1 and 2 to be intact so that cell adhesive function can occur.

THE vascular cell adhesion molecule-1 (VCAM-1)[1] plays a major role in the adhesion of leukocytes to inflamed microvascular endothelium (6, 27, 37, 45), being one of a few molecules that are induced by proinflammatory cytokines such as IL-1, TNF-α, or IFN-γ. It is involved with intercellular adhesion molecule-1 and endothelial-leukocyte adhesion molecule-1 in the transmigration and localization of lymphocytes, monocytes, eosinophils, and basophils (but not neutrophils) to sites of tissue inflammation (7, 19, 26, 44). Its interaction with these types of leukocytes appears to be via very late antigen-4 (VLA-4, $\alpha 4\beta 1$), a $\beta 1$ integrin molecule found on all four, but not on neutrophils (12). It also has been shown to interact with $\alpha 4\beta 7$ ($\alpha 4\beta P$), the lymphocyte Peyer's patch homing receptor (8, 40). VCAM-1 expression has been detected not only on cytokine-activated endothelium, but also on bone marrow stromal cells (22, 23, 41), myoblasts (39), lymphoid dendritic cells and tissue macrophages (38), rheumatoid synovium (20, 35, 47), cytokine-stimulated neural cells (4), parietal epithelial cells in Bowman's capsule, and renal tubular epithelium associated with nephritis (43, 52). It has been detected at various sites of inflammation associated with cardiac and renal allograft transplant rejection (5, 14, 29) and with acute graft versus host disease of the large intestine (25). Treatment of experimental animals with monoclonal antibodies to VCAM-1 has delayed murine cardiac allograft rejection (29, 30). Anti-$\alpha 4$ and/or anti-VCAM-1 monoclonal antibodies have been shown to block migration of lymphocytes, monocytes, and eosinophils into tissue, and to exhibit anti-inflammatory effects in animal models of experimental allergic encephalomyelitis, contact hypersensitivity reactions, and passive cutaneous anaphylaxis (1, 13, 18, 50, 53).

Structurally, VCAM-1 has been described as a member of the immunoglobulin superfamily. It is expressed on cytokine-activated endothelium as either a 110,000-mol wt transmembrane glycoprotein with seven Ig-like extracellular domains, or as alternatively spliced six or eight Ig-like domain forms (9, 16, 27, 32, 33, 37). The predominant form in the human, mouse, rat, and rabbit is reported to be the seven-domain form (9, 16, 32, 33). More recently, VCAM-1 has been seen expressed as a truncated 40,000-mol wt phospha-

Address all correspondence to Dr. Sherman Fong, Department of Immunology, Genentech, Inc., 460 Pt. San Bruno Blvd., South San Francisco, CA 94080.

1. *Abbreviations used in this paper*: anti-m-VCAM-1, anti-mouse VCAM-1; BCECF, 2',7'-bis-(2)carboxymethyl)-5(and 6)-carboxyfluorescein, acetoxymethyl ester; VCAM-1, vascular cell adhesion molecule-1; VLA-4, very late antigen-4.

tidyl inositol-linked form on endotoxin-treated lung and kidney tissues (24).

There have been recent reports that molecules comprising only the NH_2-terminal domains 1–3 were sufficient for both adhesion and costimulatory activation of T lymphocytes (10, 31). Two studies reported that the first NH_2-terminal domain and the homologous domain 4 were involved in binding to VLA-4 (28, 48). In the work presented here, we investigate the binding of a panel of secreted recombinant DNA-derived, murine VCAM-1 molecules to murine and human $\alpha4\beta1$ to elucidate the structure/function relationships for adhesion. We will show that a cluster of amino acids in domain 1 of VCAM-1 are crucial for binding to the $\alpha4\beta1$ receptor of mouse WEHI 231 and human Ramos cells.

Materials and Methods

Cloning and Expression of Murine VCAM-1

A mouse peripheral lymph node cDNA library was constructed using a cDNA library kit (lambda gt10; Invitrogen, San Diego, CA) and poly(A)$^+$ RNA isolated from murine TNF-α-stimulated mouse peripheral lymph nodes. The probe used to screen a library of ~1 million lambda gt10 bacteriophage was a random-primed (Boehringer Mannheim Biochemicals, Indianapolis, IN) full-length cDNA encoding human VCAM-1 (gift of D. Dowbenko, Genentech Inc., South San Francisco, CA). Hybridizing clones were subcloned into pBluescript (Stratagene, La Jolla, CA) and sequenced using the Sequenase Version 2.0 kit (United States Biochemical Corp., Cleveland, OH). A full-length cDNA was identified and entirely sequenced. The sequence for our murine VCAM-1 was identical to that reported by Hession et al. (17).

The cDNA for murine VCAM-1 was truncated to remove the nucleotides encoding both the transmembrane domain and the cytoplasmic tail (at amino acid residue N667) using the following primers:

Primer 1: 5'-GGAAGAATTCGCGGCCGCTTCACGTGGGC-3'
Primer 2: 5'-GGAAGTCGACCTAATGTTCTTTTCCTTTTA-3'

The 2.2-kb EcoRI-SalI PCR product was subcloned into pRK5 and expressed in human 293 embryonic kidney cells as previously reported (2). The resulting truncated murine VCAM-1 molecule was designated as MVdl-7. A 2.2-kb EcoRI-EcoRV PCR product was ligated to an EcoRV-SalI fragment encoding the hinge, CH2, and CH3 regions of murine IgG1. The resulting EcoRI-SalI fragment containing the murine VCAM-1-IgG chimera (designated MVIdl-7) was subcloned into a eucaryotic expression vector pRK5 and expressed in human 293 cells.

Purification of these proteins proceeded as follows: Serum-free conditioned medium from 293 cells expressing MVdl-7 was purified by affinity chromatography on rabbit antimurine MVdl-7-Sepharose (Pharmacia LKB Biotechnology Inc., Piscataway, NJ). MVIdl-7 was passed over protein A-Sepharose (Pharmacia, Uppsala, Sweden). Both types of molecules were eluted with 100 mM acetic acid, 500 mM sodium chloride, pH 3.0. The eluents were dripped into one-tenth volume of 1 M Tris (pH 7.5) to neutralize the samples. The samples were then dialyzed against phosphate-buffered saline, and concentrated using a pressurized stir cell (Amicon Corp., Danvers, MA.). The proteins were run on 7% SDS-PAGE to assess purity. The MVdl-7 was a monomer of 110 kD under both nonreducing and reducing conditions. The MVIdl-7 was a dimer of 230,000 mol wt under nonreducing conditions and a monomer of 115,000 mol wt under reducing conditions.

Truncated Variants of Murine VCAM-1-IgG Chimera

MVIdl-7 is composed of seven Ig-like domains. Experiments were carried out with domain truncation variants. Each domain of MVIdl-7 was sequentially truncated, starting at the COOH terminus (domain 7), to evaluate the binding function of each truncation variant. Domains in the murine molecule were defined as regions homologous to the human molecule according to Osborn et al. (27): domain 1 comprised amino acid residues Fl to I84; domain 2, H85 to L193; domain 3, Q194 to E286; domain 4, K287 to S378; domain 5, F379 to Y482; domain 6, V483 to V574; and domain 7, S575 to H666. Primers were synthesized to truncate the full-length cDNA by PCR (Perkin-Elmer Cetus Instruments, Norwalk, CT) before amino acid positions H85, Q194, K287, F379, V483, and S575. Each primer introduced restriction endonuclease sites as well as a stop codon to facilitate subcloning and expression. To aid in the purification of the truncated VCAMs, further constructs were made in which the cDNA encoding the hinge, CH2, and CH3 of murine IgG1 were ligated to each of the truncated cDNAs to generate Ig chimeras. They were designated as MVIdl, MVIdl-2, MVIdl-3, MVIdl-4, MVIdl-5, and MVIdl-6, respectively, with the wild type (WT) as MVIdl-7.

Site-directed Mutagenesis of VCAM-1-IgG Chimera

Mutations were introduced into the cDNAs encoding MVIdl-4 and MVIdl-7 by the method of Kunkel et al. (21) (Muta-Gene Phagmid In Vitro Mutagenesis Kit; Bio-Rad Laboratories, Richmond, CA) according to the manufacturer's instructions. Plasmids positive for the introduced mutations were confirmed by sequencing and expressed transiently in 293 cells. The concentration of each mutant in serum-free conditioned medium was quantified by ELISA using a goat anti-mouse IgG1 antibody as previously described (49). Mutation sites were defined using the following nomenclature: D40A describes aspartic acid mutated to an alanine at position 40.

Antibodies

HP2/1 (rat anti-human α4 chain) was purchased from Amac, Inc. (Westbrook, ME). It has been previously described and reported to bind human α4 and block lymphocyte binding to human VCAM-1 and fibronectin (36, 42). PS/2 (rat anti-mouse α4 chain-specific antibody) was obtained from the American Type Culture Collection (Rockville, MD). It has been previously reported to recognize the α4 chain of murine VLA-4 (22). Rabbit anti-mouse VCAM-1 (anti-mVCAM-1) antiserum was prepared by immunization of rabbits with recombinant derived MVIdl-7 in Freund's adjuvant. It was purified on protein A and immunoaffinity depleted of anti-mouse IgG activity on Sepharose-conjugated mouse IgG (Pharmacia LKB Biotechnology Inc.). The preparation was 0.28 mg/ml with and endpoint titer of >1:25,600 for anti-MVdl-7 and 1:158 for anti-mouse IgG by ELISA analysis. A concentration of 10 μg/ml was used in blocking experiments. It specifically blocked adhesion of WEHI 231 to 24-h TNF-α-stimulated mouse hemangioendothelioma cells, but had no effect on blocking Ramos cells binding to TNF-α-stimulated human umbilical cord vein endothelial cells (Cell Systems Corp., Kirkland, WA).

Armenian hamsters were immunized intraperitoneally with 5 μg of recombinant MVIdl-7-emulsified in monophosphoryl lipid A/trehalose dimycolate adjuvant (Ribi ImmunoChem Research, Inc., Hamilton, MT). 3 d later, the spleens from the immunized animals were fused with P3x63Ag801 myeloma cells using polyethylene glycol. Positive anti-mVCAM-1 hybridomas were screened by ELISA for binding to soluble MVdl-7. Seven monoclonal antibodies were selected and characterized. These were designated 5.7.1, 5.7.4, 5.10.8, 5.11.3, 35.1.1, 59.9.4, and 59.17.19. Clones 59.9.4 and 59.17.19 are cell adhesion-blocking monoclonal antibodies as determined by blocking of WEHI 231 or Ramos cell binding to MVdl-7. All seven monoclonal hamster anti-mVCAM-1 antibodies recognized purified recombinant MVdl-7 as a single band of ~110 kD by Western blot/SDS-PAGE under reducing conditions and by immunoprecipitation of cell extracts of murine Bend3 cells (a gift from Susan Watson, Genentech, Inc.). A hamster IgG (PharMingen, San Diego, CA) was used as a control immunoglobulin.

The hamster anti-mVCAM-1 antibodies were used to assess structural alterations in the MVIdl-4 and MVIdl-7 site-directed mutants. The 293 cell transfectant supernatants (100 μl) from the mutants were added to coats of 0.2 μg/ml goat anti-mouse IgG (Chemicon International Inc., Tecmecula, CA) on microtest wells (NUNC-Immuno Plate, MaxiSorp; Alameda Chem. & Sci., Inc., Oakland, CA) that had been blocked with 10 mg/ml of BSA in phosphate-buffered saline for 2 h at room temperature. An equivalent amount of mutant and MVIdl-4 or MVIdl-7 (WT) protein were incubated for 1 h at room temperature. 100 μl of each monoclonal hamster anti-mVCAM-1 antibody solution was added, and the microtest wells were again incubated for 1 h at room temperature. The bound hamster antibodies were detected by a 1-h incubation with goat anti-hamster IgG labeled with alkaline phosphatase at 1:2,000 dilution (Caltag Laboratories, South San Francisco, CA). The enzyme activity was detected with 1 mg/ml of *p*-nitrophenyl phosphate, disodium (Sigma Chemical Co., St. Louis, MO), in 50 mM carbonate, 10 mM $MgCl_2$ for 30 min at room temperature. The optical density at 405 nm was recorded on a microplate reader (Molecular Devices Corp., Menlo Park, CA).

Two blocking rat anti-mVCAM-1 antibodies were used for binding studies and for the assessment of changes to gross structure. The M/K-2.7

was obtained from the American Type Culture Collection. It has been described as a blocking antibody for the binding of human lymphoma cells to mouse endothelial cells (23). MVCAM.A429 was obtained from PharMingen.

Cell Adhesion Assay

Recombinant MVdl-7 and MVIdl-7 were precoated onto separate microtest wells (NUNC-Immuno Plate, MaxiSorp) at 1 μg in 100 μl/well for 1 h at room temperature. The wells were quenched with RPMI 1640 containing 5 mg/ml BSA. The test cells were labeled with 2',7'-bis-(2-carboxyethyl)-5(and-6)-carboxyfluorescein, acetoxymethyl ester (BCECF) from Molecular Probes (Eugene, OR) for 30 min at 37°C according to the method of Gimbrone et al. (15). The labeled cells were suspended at 4×10^6 cells/ml in RPMI 1640 containing 5 mg/ml BSA. Test cells were incubated with immobilized MVdl-7, or MVIdl-7, at 37°C for 15 min. The nonadherent cells were removed by centrifugation of the sealed microtest plate in the inverted position at 200 *g* for 5 min. The supernatant was aspirated. The bound cells were solubilized with 0.1% SDS in 50 mM Tris/HCl, pH 8.5. The proportion of adherent cells was determined for each well by measuring the amount of released fluorochrome from lysed cells on an analyzer (Fluorescence Concentration Analyzer; Pandex, Mundelein, IL) set at 485-nm excitation and 535-nm emission wavelengths. Adherence was also performed on microwells precoated with human fibronectin (Sigma Chemical Co.).

For the test of MVIdl-4 and MVIdl-7 site-directed mutants in the adhesion assay, serum-free culture supernatants from 293 cell transfectants were serially added to microwells that had been coated with 200 ng/well goat anti-mouse IgG1 (Caltag Laboratories) and quenched with 5 mg/ml BSA. Supernatants were incubated for 2 h at room temperature. For the assessment of the amount of each mutant protein captured on the microwells, an alkaline phosphatase–labeled goat anti-mouse IgG1 (Caltag Laboratories) at 1:1,000 dilution was added, and wells were incubated for 1 h at room temperature. The enzyme activity was detected with *p*-nitrophenyl phosphate disodium, taking optical density readings at 405 nm. The sensitivity of this capture assay was such that protein concentration determinations and cell binding analysis of mutants could be made within the concentration range of 20–150 ng/ml.

The cell adhesion assay described above was repeated with the following variation for both MVIdl-4 and MVIdl-7. For the assessment of Ramos cell binding to mutant MVI, BCECF-labeled cells were added as above. For WEHI 231 cell binding, a rat anti-mouse FcγRII antibody (PharMingen) at 2 μg/10^6 cells was added to block binding through the Fc receptor (46). To block the binding of WEHI 231 cells through the cell-surface IgG to the goat anti-mouse IgG1 precoat, 2 μg/ml of mouse IgG1 (Calbiochem, San Diego, CA) was added to the assay medium.

Model of Murine VCAM-1 Domain 1

A model of MVd1 was based on the crystal structure of a human IgG CH1 domain (11). Alignment of the MVd1 sequence with CH1 (Fig. 1) was performed manually using C23, C71, W35, S54, and the requirement for hydrophobic residues at buried positions to guide the alignment. In human CH1, the W35 sidechain forms a hydrogen bond with the S54 sidechain; this was retained in the MVd1 model. Insertions and deletions in MVd1 relative to human CH1 occur in the loops connecting the β strands. In addition, β strands D and E are shorter in MVd1 (Fig. 1).

CH1 was transformed into MVd1 in two steps. First, all residues except those involving insertions or deletions were changed to the MVd1 sequence using the INSIGHT-II program (Biosym Technologies, San Diego, CA). Where possible, conformations of MVd1 sidechains were kept similar to those of CH1; otherwise, they were based on rotamer libraries (34), packing, and hydrogen bonding considerations. Second, loop structures containing the MVd1 insertions or deletions were gleaned from searches of the Protein Data Bank (3) crystal structures using the INSIGHT-II program. Several loop conformations were possible for each new loop, and in each case, the choice was based on the nature of the MVd1 amino acids. The loop connecting β strands C and D (loop CD) is relatively large (10 residues) and several loop conformations were evaluated.

The MVd1 model was subjected to energy minimization using the DISCOVER program (Biosym Technologies). The all-atom AMBER forcefield (51) was used for all calculations, using a 14-Å cutoff for nonbonded interactions and a linear dielectric ($\epsilon = 4.0$*r). Before minimization, hydrogen atoms were added to the structure using INSIGHT-II, and positions of hydrogens on serine, threonine, and tyrosine sidechains were checked visually for proper alignment in hydrogen bonds, if present. Energy minimization was performed in three stages. In stage one, 500 cycles of steepest-descents minimization were used. 46 hydrogen bond constraints (50 kcal/mol) were also invoked: 37 mainchain-mainchain, 8 mainchain-sidechain, and 1 sidechain-sidechain hydrogen bonds. This allowed new loop structures and all sidechains to move while preserving the integrity of the CH1 protein fold. In stage two (1,000 cycles), conjugate-gradient minimization was used. In stage three (5,690 cycles), the hydrogen bond constraints were released, and the minimization continued until the maximum derivative was <0.01 kcal/mol-Å.

```
                β-strand A          β-strand B     β-strand C
                 • •#•# •            •#•#•#•# •     • • •
humCH1      KGPSVFPLAPSSKSTSGGT-AALGCLVKDYFPEPVTVSWNSGALT
muVCAM-D1   FKIEISPEYKTIAQIGDSMALTCSTTGCES--PLFSWRTQIDS
ratVCAM-D1  FKIEISPEYKTLAQIGDSMLLTCSTTGCES--PSFSWRTQIDS
huVCAM-D1   FKIETTPESRYLAQIGDSVSLTCSTTGCES--PFFSWRTQIDS
            1       10        20        30          40

                β-strand D  β-strand E        β-strand F
                 *#*#*#      •#•#•#•#• • •     • • • •
humCH1      SG--VHTFPAVLQSSGLYSLSSVVTVPSSSLGTQ-TYICNVNH
muVCAM-1    PLNAKVRTEGS---------KSVLTMEPVSFENEHSYLCTATC
ratVCAM-1   PLNGKVKTEGA---------KSVLTMDPVSFENEHSYLCTATC
huVCAM-1    PLNGKVTNEGT---------TSTLTMNPVSFGNEHSYLCTATC
                   50                  60        70

                β-strand G
                  * * *
humCH1      KPSNTKVDKKVEPKSC
muVCAM-1    GS--GKLERSIHVDIY
ratVCAM-1   NS--GKLERGIQVDIY
huVCAM-1    ES--RKLEKGIQVEIY
                80
```

Figure 1. Alignment of human, rat, and murine VCAM-d1 with human IgG CH1. β strands in human IgG CH1 crystal structure and mVCAM-d1 model are underlined. Residues in the human IgG CH1 crystal structure are denoted as buried (•), partially buried (*), or at the CH1-CL interface (#).

Results

Cell Binding to Immobilized Recombinant Murine VCAM-1 (MVdl-7) and Murine VCAM-1–IgG (MVIdl-7)

Two secreted, soluble, and recombinant forms of murine VCAM-1 exhibited binding specificity to $\alpha4\beta1$-positive lymphoid cells. BCECF-labeled murine WEHI 231 and human Ramos cells bound to both MVdl-7 and MVIdl-7 above the basal level binding that they exhibited with BSA (Fig. 2, *A* and *C*). The binding of the murine and human cells was inhibited by PS/2 (anti-murine $\alpha4$ subunit antibody) and HP2/1 (anti-human $\alpha4$), respectively, but not by a rat IgG2b isotype control antibody (Fig. 2, *B* and *D*). A rabbit antimurine VCAM-1 antiserum also inhibited binding. This binding

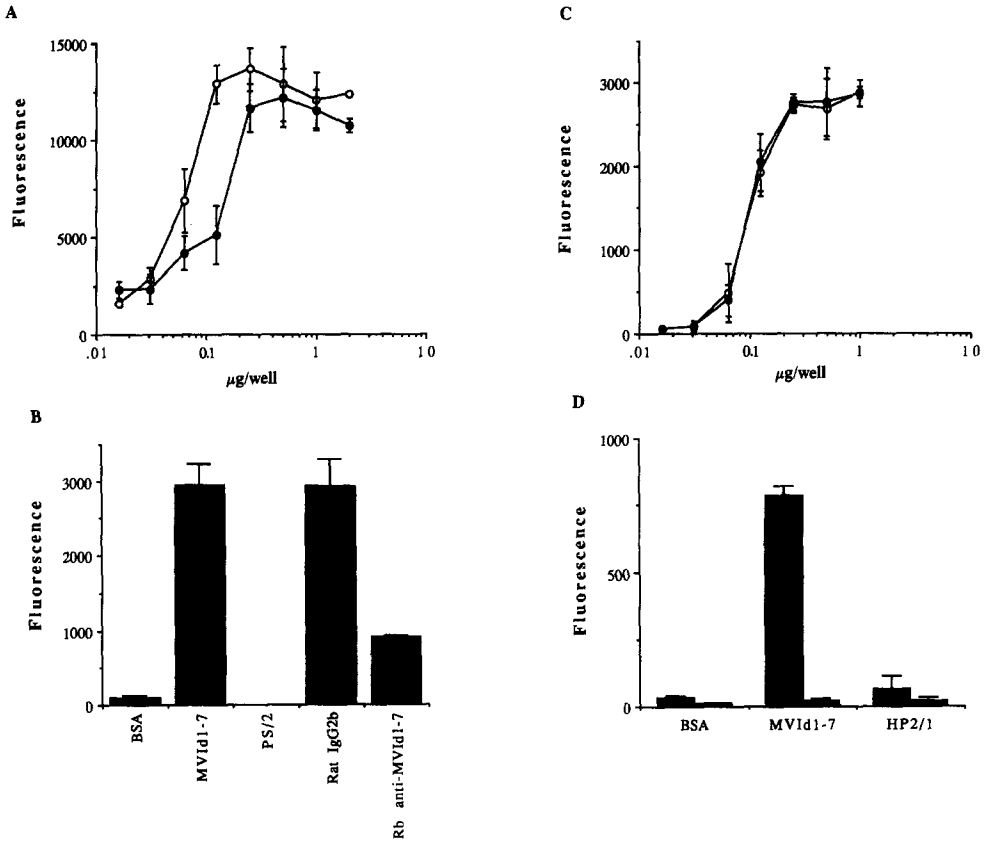

Figure 2. Binding of BCECF-labeled murine WEHI 231 and human Ramos cells to microwells precoated with varying concentrations of recombinant soluble MVd1-7 (●) and MVId1-7 (○). Binding is expressed as fluorescence units ± SD. (*A*) WEHI 231 and (*C*) Ramos. (*B*) The binding of WEHI 231 to MVId1-7 is inhibited by anti-α4 antibodies PS/2 (10 μg/ml). (*D*) The binding of Ramos to MVId1-7 (■) is inhibited by HP2/1 (10 μg/ml). K562, α4-negative cell (▨). The peak binding fluorescence for WEHI 231 represents an average of 76 ± 4% (SD) of the input cell number (2×10^5 cells/well). The peak binding by Ramos cells represents 38 ± 13% (SD) of input number of cells.

is therefore α4β1/VCAM-1 dependent. This same pattern of binding, with inhibition by anti-VCAM-1 antiserum, was seen when rat splenocytes and rabbit peripheral lymphoid cells were the source of α4 (data not shown). We have seen similar binding by human α4-positive Jurkat T cells (data not shown). The α4-negative control cell line K562 did not bind to precoated MVId1-7. The Ramos and K562 cells bear surface FcγRII receptors, therefore, the binding of the MVId1-7 is not caused by interaction via the Fc domain of the fusion protein.

These data showed that the recombinant soluble molecules MVd1-7 and MVId1-7 were functionally active, similar in their interaction with the homologous mouse VLA-4 receptor, and cross-reactive with VLA-4 from several other different animal species, including humans.

Binding of Cells and Anti-VCAM-1 Monoclonal Antibodies to Truncated Variants of MVId1-7

The first two NH_2-terminal Ig-like domains on murine VCAM-1 were both necessary and sufficient for binding to murine WEHI 231 and human Ramos cells. Domain deletion mutants, expressed as chimeric IgG molecules in serum-free conditioned media, were captured on separate microwells precoated with goat anti-mouse IgG antibody and presented to cells at 0.23 nM. This concentration had previously been determined to be saturating for all variants by an immunoassay under the antibody capturing condition. As illustrated in Fig. 3, *A* and *B*, variant chimeric fusion molecules composed of the first two or more of the seven Ig-like domains of VCAM-1 were sufficient to bind both WEHI 231 and Ramos cells. The variant MVId1, composed of only the first domain of VCAM-1 fused to the hinge, CH2, and CH3 domains of IgG heavy chain, was not capable of binding cells, even at a molar concentration 30-fold higher than the other mutants. MVId1 was inactive. The supernatant fluids from the background control pRK5 mock transfectant 293 cells added to the goat anti-mouse IgG precoat did not exhibit cell binding.

The binding by Ramos cells to the MVI variants could be inhibited totally by monoclonal hamster anti-mVCAM-1 (clone 59.17.19), but not by normal hamster IgG (Fig. 3 *C*). Inhibition was also observed for another monoclonal hamster anti-mVCAM-1 (clone 59.9.4) and two commercially available blocking rat anti-mVCAM-1 antibodies tested, M/K-2.7 (23) and MVCAM.A429. No blocking of cell adherence was observed for five other hamster anti-VCAM-1 monoclonal antibodies tested (clones 5.7.1, 5.7.4, 5.10.8, 5.11.3, and 35.1.1; data not shown). The cell binding was inhibited by PS/2 for mouse cells and HP2/1 for human cells, but not by equivalent concentrations of a rat IgG2b or mouse IgG1 control antibody respectively (data not shown). These data suggest that the NH_2-terminal domains 1-2 of the recombinant murine VCAM-1-IgG are sufficient for binding to either WEHI 231 or Ramos cells.

In corroboration, blocking monoclonal antibodies (59.9.4, 59.17.19, M/K-2.7, and MVCAM.A429) were observed to bind to truncated murine VCAM-1-IgG molecules bearing, at minimum, the first two NH_2-terminal Ig-like domains, MVId1-2 to MVId1-7 (Table I). Nonblocking monoclonal antibodies bound to MVId1-3 through MVId1-7, but not to MVId1-2. None of the antibodies tested bound to MVId1. These results support the hypothesis that the structures

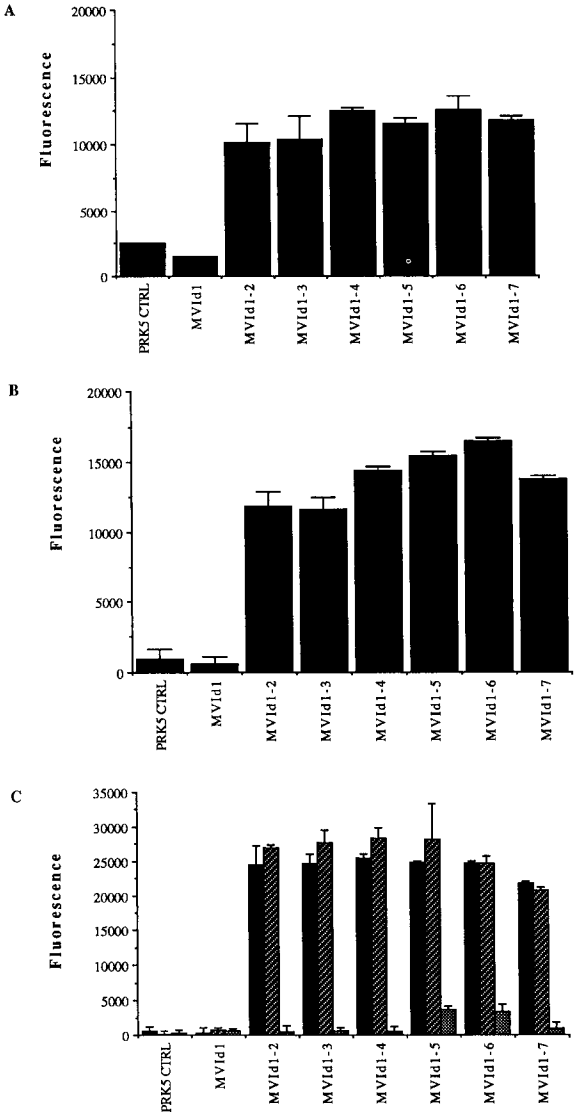

Figure 3. Cell binding to truncated versions of murine VCAM-1-IgG derived from 293 cell transfection culture supernatants. VCAM-1-IgG variants were captured at ~0.23 nM on microwell precoats of goat anti-mouse IgG (1 μg/ml). PRK5 CTRL denotes a 293 cell mock transfection supernatant. Binding is expressed as fluorescence units ± SD. (*A*) WEHI 231, (*B*) Ramos, and (*C*) Ramos cell binding is blocked by 10 μg/well of hamster anti-mVCAM-1 antibody (▩), but not by 10 μg/well of hamster IgG (▨).

Table II. MVId1-4 Mutant Binding Summary

	Binding to cells		
	α4β1 WEHI 231*	α4β1 Ramos*	Transfectant expression‡
WT (MVId1-4)	+	+	+
293 Mock control	−	−	−
Domain 1			
E8A	+	+	+
K10A	+	+	+
D17A	+	+	+
E29A	ND	−	−
S34A	ND	+	+
R36A	−	−	+
T37A	+	+	+
Q38A	ND	−	−
D40A	−	−	+
D40K	−	−	+
N44A	+	+	+
K46A	+	±	+
R48A	+	+	+
E50A	+	+	+
S54A	−	−	+
T57A	+	+	+
E59A	+	+	+
E64A	+	+	+
N65A	+	−	+
E66A	+	+	+
H67A	ND	−	−
L70A	ND	−	−
T72A	±	−	+
K79A	+	+	+
E81A	+	−	+
R82A	+	+	+
H85A	+	+	+

* Cell binding key: +, >80% of WT; ±, <50% of WT; −, <10% no binding; ND, not done. ‡ Determined by anti-IgG ELISA: +, expression; −, no expression.

sufficient for adherence reside within the first two NH_2-terminal domains.

Specific Amino Acid Residues on Domain 1 of MVId1-4 and MVId1-7 Are Required for Cell Binding

A series of soluble MVId1-4 mutants with L-alanine or L-lysine substitutions in domain 1 residues was expressed in 293 cells to test whether the first domain alone was sufficient

Table I. The Binding of Monoclonal Hamster and Rat Anti-Murine VCAM-1 to Truncated VCAM-1 IgG

	OD at 405 nm							
mAb	293	MVId1	MVId1-2	MVId1-3	MVId1-4	MVId1-5	MVId1-6	MVId1-7
5.7.1	0.199	0.226	0.159	0.53	0.596	0.605	0.647	0.634
5.7.4	0.301	0.278	0.241	0.657	0.669	0.693	0.748	0.631
5.10.8	0.197	0.213	0.175	0.59	0.593	0.594	0.685	0.437
5.11.3	0.246	0.232	0.213	0.575	0.596	0.585	0.624	0.526
35.1.1	0.152	0.151	0.144	0.451	0.444	0.453	0.48	0.438
59.9.4	0.162	0.154	0.668	0.72	0.747	0.743	0.711	0.583
59.17.19	0.334	0.296	0.643	0.63	0.632	0.696	0.653	0.502
M/K-2.7	0.044	0.071	0.357	0.339	0.315	0.345	0.365	0.452
MVCAM.A429	0.017	0.036	0.835	0.854	0.872	0.901	0.904	0.977

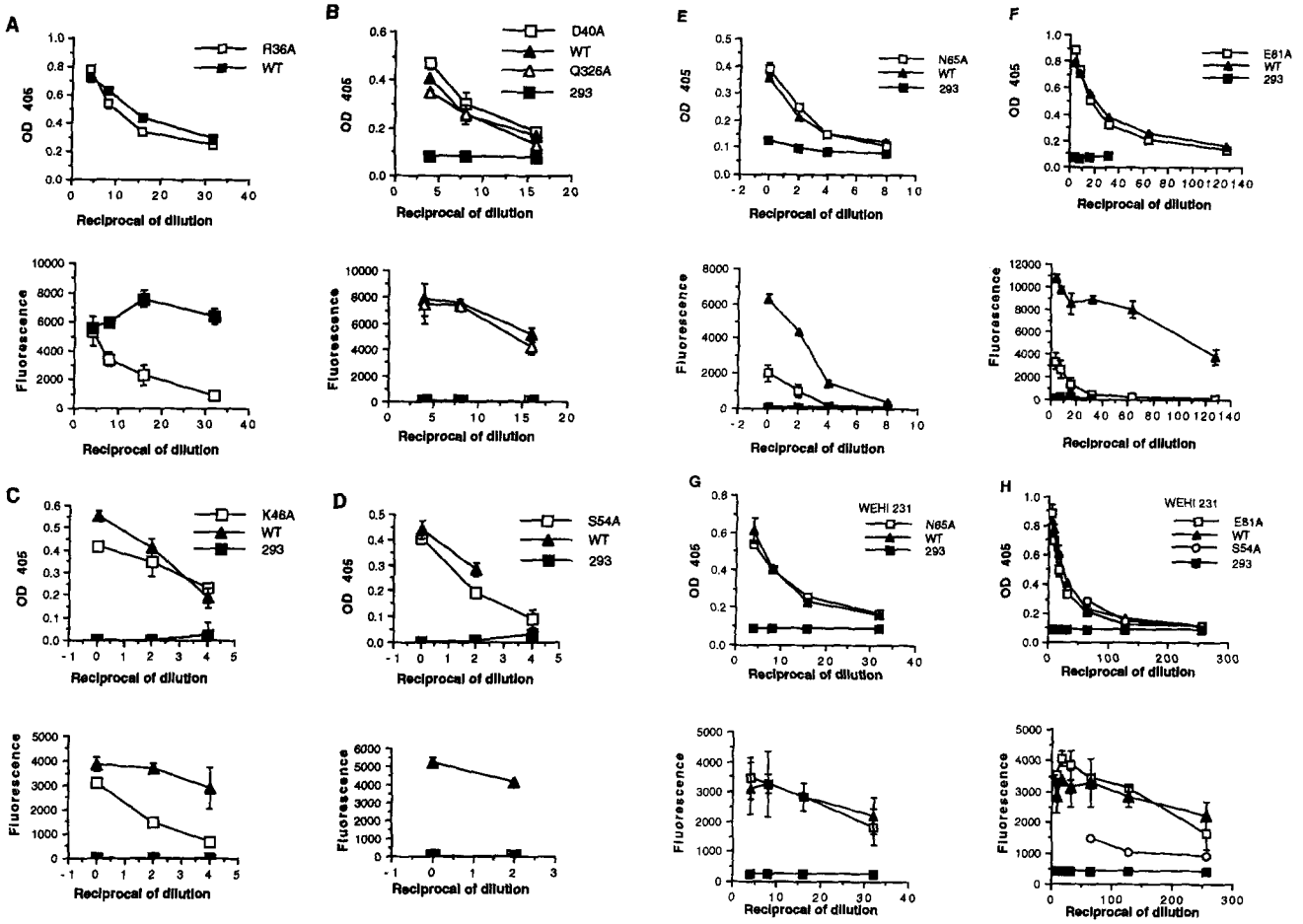

Figure 4. Alanine substitutions at specific amino acid residues in domain 1 of MVIdl-4 that affected Ramos cell binding are illustrated. MVIdl-4 mutant supernatants derived from 293 cell transfections were serially diluted and added to microwells coated with goat anti-mouse IgG. Equivalent concentrations of mutants and MVIdl-4 (WT) were used in the adherence assay as shown by relative OD405 values determined for serial dilutions of mutants and WT captured on the anti-IgG-coated microwell (illustrated in the top panels of *A–J*). The R36A and D40A mutant supernatants contained ~160 ng/ml (1:4) of anti-IgG-reactive protein as compared to MVIdl-4. The K46A mutant contained 160 ng/ml (neat). S54A contained ~40 ng/ml. The N65A mutant contained 300 ng/ml (1:2 dilution) and the E81A mutant contained 640 ng/ml at 1:2 dilution). The T72A mutant and the K10A mutant were at 160 ng/ml each at 1:2 dilution. The binding of BCECF-labeled Ramos cells is recorded as relative fluorescence ±SD (bottom panels of *A–F*, *I* and *J*). The binding of WEHI 231 is similarly reported (bottom panels of *G* and *H*). The binding is compared to the negative control PRK5 mock transfection 293 cell culture supernatant or as in *B*, to the mutation Q326A.

for adhesive function. The mutants are listed and the cell binding data is summarized in Table II. The concentrations of mutant MVIdl-4 molecules tested ranged from 40 to 640 ng/ml, as determined by comparison to a purified MVIdl-4 standard. A mock pRK5 vector transfectant supernatant from human 293 cells was used as a background control.

Ramos and WEHI 231 cells exhibited no binding to D40A, D40K, and S54A mutants as compared to equivalent concentrations of the wild type MVIdl-4 molecule or to mutant Q326A. Representative binding curves for D40A and S54A are shown in Fig. 4, *B* and *D*, respectively. The lack of binding by Ramos cells to the D40K mutant was identical to that observed for D40A (data not shown). Based on a computer-generated model of domain 1 (Fig. 5), the D40 residue is associated with a β turn between β strands C and D. Mutation of this hydrophilic residue should not greatly perturb the

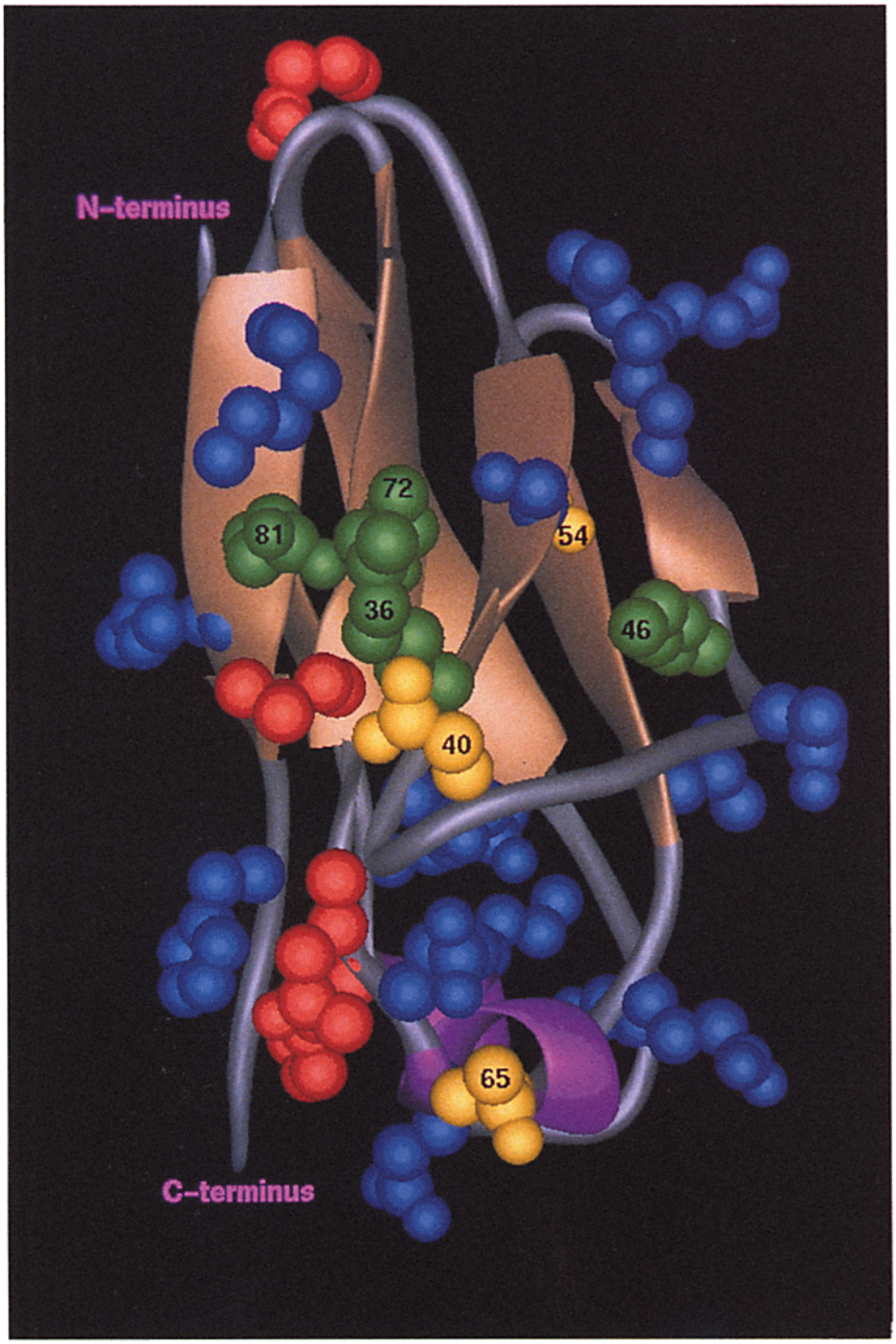

Figure 5. Computer-generated model of the first domain of murine VCAM-1. β strands are shown as beige-colored ribbons; α-helix (loop EF and part of loop AB) is in purple. Relevant sidechains tested for their effect on binding are colored as follows: blue, no effect; green, partial reduction; yellow, complete reduction; and red, protein not expressed. Residue numbers are provided for sidechains that had a complete or partial reduction in binding. This figure was drawn using MIDAS (University of California, San Francisco).

structure of the molecule. For comparative purposes, the K10 residue is located within a loop connecting two β strands A and B. Mutation to K10A did not disrupt the binding by WEHI 231 or Ramos cells (Fig. 4 *J*), nor did it induce gross structural changes (Table III).

This stands in contrast to the S54A mutation, which did result in reduction of cell adherence and of the binding of nonblocking and blocking antibodies (Table III). Binding by blocking antibodies was reduced by 83–93%, while that of nonblocking antibodies was reduced by 24–53%. Based upon the computer model, S54A is likely buried within β strand E and forms a hydrogen bond with W35 (Figs. 1 and 5) and thus is essential for the structural integrity of the molecule.

Alanine substitutions at R36, K46, T72, and E81 also resulted in reduced binding of Ramos cells (Table II and Figures 4, *A*, *C*, *I*, and *F*, respectively). All four of these residues seemed to be structurally important. R36 is next to W35, which is hydrogen bonded to S54. The importance of this bond is also borne out by mutation of S34, which simi-

Table III. Anti-VCAM-1 Antibody Binding to MVId1-4 Mutants

		mAb Anti-VCAM-1 binding to mutants (% of binding to WT)								
							Blocking mAb			
	Mutant expression	5.7.1	5.7.4	5.10.8	5.11.3	35.1.1	59.9.4	59.17.19	M/K-2.7	MVCAM.A429
WT (MVId1-4)	+	100	100	100	100	100	100	100	100	100
293 Mock control	−	0	00	0	0	0	0	0	0	0
Domain 1										
E8A	+	98	102	101	104	104	68	61	123	105
K10A	+	100	120	96	103	109	100	104	97	103
D17A	+	97	98	98	92	94	89	84	108	109
E29A	−	0	0	0	0	0	0	0	ND	ND
S34A	+	69	70	72	60	65	62	70	51	41
R36A	+	79	78	80	76	81	76	73	71	42
T37A	+	61	54	66	60	59	63	66	50	59
Q38A	−	0	0	0	0	0	0	0	ND	ND
D40A	+	116	110	117	118	113	112	115	102	2
D40K	+	96	102	97	94	96	78	95	86	0
N44A	+	102	137	110	106	121	113	98	88	97
K46A	+	123	106	128	108	126	126	111	89	92
R48A	+	94	86	93	85	86	82	80	88	97
E50A	+	84	110	104	98	106	94	93	100	94
S54A	+	64	52	76	58	47	9	7	12	17
T57A	+	57	36	58	51	58	53	45	53	53
E59A	+	80	74	83	77	82	80	82	86	87
E64A	+	97	105	98	97	104	97	97	101	110
N65A	+	68	63	63	61	61	39	36	80	77
E66A	+	103	115	96	106	106	97	91	105	107
H67A	−	0	0	0	0	0	0	0	ND	ND
L70A	−	0	0	0	0	0	0	0	ND	ND
T72A	+	72	60	80	69	70	77	87	73	71
K79A	+	101	95	96	94	91	104	105	88	101
E81A	+	95	98	96	92	97	95	86	91	73
R82A	+	107	96	97	103	91	99	106	103	106
H85A	+	83	69	83	66	78	62	59	85	64

larly disrupts antibody binding, but not cell adherence. The R36A mutation had a profound effect on the binding of the blocking anti-VCAM-1 antibody MVCAM.A429. K46 is predicted to be within β strand D and partially buried. E81 is predicted to be within β strand G adjacent to R82, which is partially buried. T72 is on β strand F positioned between two buried residues C71 and A73, and might therefore be expected to reduce cell binding.

Of particular interest is the finding that the degree of reduction in cell binding to the R36, K46, T72, and E81 mutants was highly dependent on the concentration at which they were precoated on the microwells. Higher concentrations resulted in better binding, while lower concentrations resulted in poorer binding, as compared to equivalent concentrations of the wild type molecule. These data suggest that while the mutations could disrupt cell adhesive function, binding could be augmented by increasing the avidity of the interaction or the number of molecules interacting.

In general, the mutations that affected Ramos cell binding also affected the binding to WEHI 231 cells. However, three mutants, K46A, N65A, and E81A, exhibited reduced binding by Ramos cells while exhibiting little or no effect on WEHI 231 cell binding. Representations of N65A and E81A are shown in Fig. 4, *G* and *H*. The N65A mutation completely reduced the binding of Ramos cells, while K46A and E81A only partially reduced binding. These results raise the possibility that there may be species differences in the recognition residues on MVId1-4.

Alanine substitutions at E8, K10, D17, T37, N44, R48, E50, T57, E64, E66, K79, R82, and H85 did not alter binding by either Ramos or WEHI 231 cells (Table II). There was no yield for the three mutations, E29A, H67A, and L70A.

To further test whether a mutant at D40 in the MVId1-7 molecule could also exhibit reduction in binding, a panel of mutants comprised of mutations D40A, D40E, D40K, and D40N were prepared. The mutants D40A, D40K, and D40N, tested at comparable molar concentrations to wild type MVId1-7, reduced binding to background levels. The D40E mutation did not affect binding (Fig. 6). The effect of mutation on D40 was not unique to Ramos or WEHI 231 cell binding. The human Jurkat T cell line binding to D40A, D40K, and D40N MVId1-7 mutant molecules was also completely inhibited (data not shown). These data are consistent with the idea that a change of a single amino acid residue, D40 in domain 1 of the MVId1-7 molecule, to a residue with either an aliphatic, basic, or amide sidechain is sufficient to completely abrogate its binding by $\alpha 4$ positive cells. An acidic sidechain composed of D40 or E40 was sufficient for binding.

Mutation of MVId1-4 at positions D317A, R324A, Q326A,

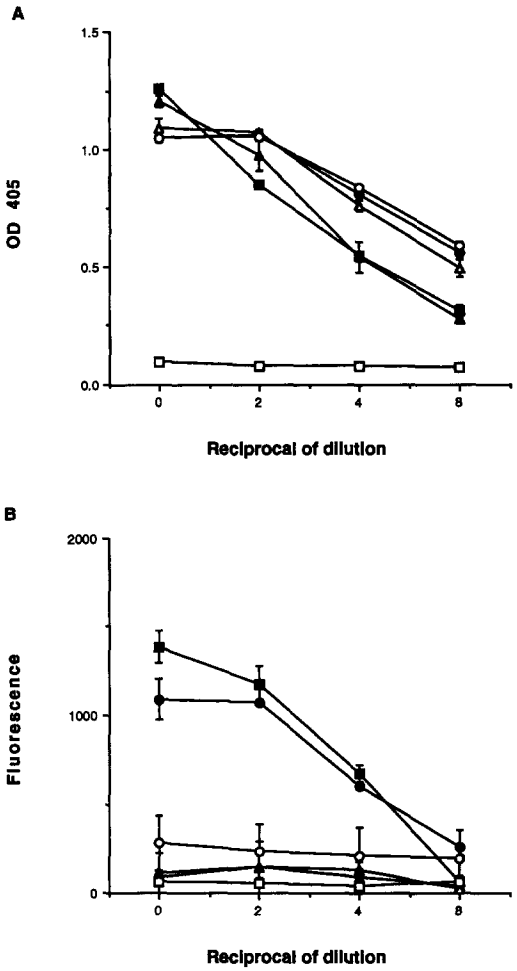

Figure 6. Ramos cell binding to mutants of MVId1-7 or MVId1-7 (WT) derived from 293 cell transfections. (*A*) Mutants captured at equivalent concentrations as determined by ELISA analysis as in Fig. 4. (*B*) Ramos cell binding as determined by fluorescence ± SD. The binding to 293 mock transfection supernatant is shown as a negative control. -■-, WT; -▲-, D40A; -●-, D40E; -△-, D40K; -○-, D40N; -□-, 293.

D328A, R336A, E338A, and K341A in the fourth Ig-like domain did not result in reduced binding by Ramos or WEHI 231 cells (data not shown). These results suggest that the fourth domain does not contribute to adhesive function in MVId1-4.

Specific Amino Acid Residues on Domain 1 of MVId1-4 Are Required for the Binding of Neutralizing Hamster and Rat Anti-mouse VCAM-1 Monoclonal Antibodies

An analysis of the binding of a panel of adhesion-blocking and nonblocking hamster anti-VCAM-1 monoclonal antibodies was carried out to test whether the same amino acid substitutions that perturb cell adherence can result also in altering antibody binding or whether specific mutations induced gross structural perturbations in the molecule. Comparative data on the antibodies binding to mutants, relative to wild type are summarized in Table III.

Alanine substitution at E8 reduced the binding of two blocking antibodies, clones 59.9.4 and 59.17.19, to 68 and 61% of wild-type binding, respectively. There were no measurable differences in the binding by nonblocking antibodies to E8 and wild type. E8A had no impact on the binding of WEHI 231 or Ramos cell binding. The D17A mutation also slightly reduced blocking antibody binding (to 87 ± 4% of wild type) without exhibiting any effect on nonblocking antibody binding or cell adhesion. The data suggest that the residues E8 and D17 are crucial for binding by blocking antibodies 59.9.4 and 59.17.19, but not for cell adhesion or other anti-VCAM-1 antibodies.

The mutation R36A reduced the binding of both blocking and nonblocking antibodies to a range of 73-81% of wild-type binding (average of 78%). In the experiments shown above, this mutation also resulted in reduced binding by both WEHI 231 and Ramos in a mutant dose dependent manner (Fig. 4). The results suggest that this mutation may induce a subtle change in the conformation of the molecule, thereby impacting both antibody binding and adhesion.

The D40 residue was observed to be key to cell adherence. Anti-VCAM-1 antibody-binding data suggested that the D40A and D40K mutations did not result in gross structural perturbations (Table III). Only the binding of one blocking anti-VCAM-1 antibody (MVCAM.A429) was completely abrogated by the D40A and D40K mutations. The inference is that D40 is one residue crucial for cell adherence and binding by the blocking anti-VCAM-1 monoclonal antibody MVCAM.A429.

Both blocking and nonblocking antibodies showed reduced binding to mutants S54A and N65A as compared to wild type. S54A profoundly reduced the binding of blocking antibodies to 8 ± 1% (SD) of wild type and the binding of nonblocking antibodies to 59 ± 11% of wild type. The S54A mutation also inhibited the adherence of both WEHI 231 and Ramos. Similarly, the N65A mutant reduced blocking antibodies to 38 ± 2% and nonblocking antibodies to 63 ± 3%. Both of these mutations seem to more profoundly reduce blocking antibody binding than nonblocking antibody binding, thus suggesting that these residues influence the structural integrity of the molecule, but also contribute significantly to cell adhesive function.

In summary, alanine substitution of three residues (R36, S54, and N65) can partially affect the gross structure of mVCAM-1, as exemplified by their perturbation of anti-VCAM-1 antibody binding. These data are consistent with their effect on cell adhesion. Alanine substitution at E81 affected the binding of blocking antibody MVCAM.A429 only, with alteration at E81 causing reduction in binding by Ramos cells. Two residues, E8 and D17, seem to be associated with the binding of the two blocking anti-VCAM-1 antibodies, while having no direct influence on cell adhesion. D40A, the mutation with the most profound effect on cell adhesion, produced a measureable effect on the binding of only one blocking antibody, MVCAM.A429.

Discussion

We have shown that recombinant soluble mVCAM-1 molecules, secreted by human 293 cells either as a truncated molecule without the transmembrane and cytoplasmic tail domains, or as an IgG fusion molecule, exhibited cell adhesive functions similar to those previously reported for cell mem-

brane expressed forms of human VCAM-1. The binding was through the lymphocyte $\alpha 4\beta 1$ receptor. Both murine WEHI 231 and human Ramos cells binding to immobilized MVdl-7 or MVIdl-7 could be inhibited by antibodies to either $\alpha 4$ or VCAM-1.

The secreted MVIdl-7 molecule could be truncated to a smaller molecular form, composed of the first two NH_2-terminal domains, that retained cell adhesive function comparable to that of MVIdl-7. Pepinsky et al. (31) reported that a soluble truncated form of human VCAM-1 derived from COS cells and composed of the first two domains was bound by Ramos cells. However, the binding was not inhibited by anti-VCAM-1 antibody 4B9. In our investigation, the binding of WEHI 231 and Ramos cells to MVIdl-2 was totally inhibited by monoclonal hamster anti-mVCAM-1 antibodies 59.9.4 and 59.17.19. This minor difference may be explained by our use of a different monoclonal anti-VCAM-1 antibody or by the study of VCAM-1 derived from murine as opposed to human origin.

By alanine substitution of acidic and basic charged amino acid residues in the first domain, the D40 residue was found to strongly inhibit binding by both WEHI 231 and Ramos cells. A requirement for an acidic sidechain at amino acid residue 40 was evident with the D40E mutation showing no impact on cell binding, while D40A, D40K, and D40N inhibited binding. Alteration of the D40 residue in both the MVIdl-4 and the MVIdl-7 version of the soluble mVCAM-1 molecule led to complete loss of cell binding. Experimentally, the loss of adhesive function was not accompanied by global molecular structural perturbations, as tested by the binding of blocking or nonblocking hamster VCAM-1 antibodies. The location of D40 on a hydrophilic loop between β strand C and D of the VCAM-1 molecule suggests that this residue might interact directly with $\alpha 4\beta 1$ receptors. Its location is a region corresponding to the second complementarity determining region of immunoglobulins.

In our investigation, the D40A mutation alone in domain 1 of MVIdl-7 completely inhibited cell adhesiveness. Arguably, the first domain may make the greatest contribution to binding by our recombinant soluble VCAM-1 molecule. In our hands, mutation of MVIdl-4 at positions D317A, R324A, Q326A, D328A, R336A, E338A, and K341A did not result in reduced binding by Ramos or WEHI 231 cells, suggesting that domain 4 is not required for adhesive function. This would appear to be in conflict with the report by Osborn et al. (27), who showed that the fourth domain may have cell adhesive function. These investigators observed that a COS cell expressing the alternatively spliced six Ig-like domain form of human VCAM-1 was bound by Ramos cells. However, in their VCAM-1 molecule, the first domain was swapped for the fourth domain. Their results and ours are therefore complementary.

A second mutation involving S54A also reduced binding, probably by disrupting the hydrogen bonding that normally occurs between S54 and W35, as predicted by the computer model illustrated in Fig. 6. The S54A mutation inhibited both blocking and nonblocking anti-VCAM-1 antibody binding with the effect being greater on blocking antibodies. The results suggest that the mutation most likely changed the local conformational structure of the molecule. If so, it follows that S54 would influence both cell adhesion and antibody binding.

There were two distinct patterns seen in the loss of cell binding to the mutants. The mutations D40A, S54A, and N65A abrogated cell adherence at all concentrations of mutants tested, whereas the R36A, K46A, and E81A mutations exhibited cell binding at higher precoat concentrations, but not at lower mutant precoat concentrations. A possible explanation for the former observation is that the mutations D40 and S54 sufficiently reduced the affinity of the interaction so that increasing the mutant precoat concentrations did not lead to an increase in the avidity of the interaction. On the other hand, the R36A mutant had a lower affinity interaction that was overcome by increasing the precoat concentrations. These results strongly support the hypothesis that the D40 and S54 residues are crucial for maintaining adhesive function. These residues are conserved in the mouse, rat, and human VCAM-1 molecules.

The R36 and D40 residues are adjacent to four other altered residues that exhibited an influence on cell adhesion, mutations K46A, N65A, T72A, and E81A. The K46A, N65A, and E81A mutations inhibited partially or completely the binding by Ramos cells, while displaying no modification of the binding by WEHI 231 cells. Possible explanations are (*a*) that homologous interactions between mouse cell and mouse protein may be of higher affinity than the heterologous ones between human cell and mouse protein; or (*b*) that the structures on MVIdl-4 involved in the binding to Ramos cells may be slightly different from those for binding to WEHI 231. Interestingly, these three residues are adjacent conformationally to R36 and D40. All are clustered within the same region of the molecule and are conserved among mouse, rat and human VCAM-1 sequences, suggesting their importance for cell adhesive function.

Only two residues were observed to block antibody association without contributing to cell adhesion. Alanine substitution at two residues, E8 and D17, were able to inhibit blocking antibody binding, but induced no effect on the binding by Ramos or WEHI 231 cells. Based on the computer model, these two residues are both located in the loop between β strand A and B (shown at the right hand bottom corner of Fig. 5). These residues are not in close proximity to the residues influencing cell adhesion.

Of the residues that did not affect binding either to Ramos or WEHI 231 cells, those at positions K10, R48, E64, and R82 differ in sequence between human, rat, and murine VCAM-1. This suggests that these positions are not involved in species specific interaction even though R48, E64, and R82 are adjacent to residues that did affect binding.

In summary, by site-directed mutagenesis of a secreted soluble recombinant murine VCAM-1 molecule, we have identified amino acid residues that influence both cell adhesion and binding by blocking monoclonal anti-VCAM-1 antibodies. In particular, the D40A mutation resulted in complete inhibition of both cell adhesive function and binding by blocking antibody MVCAM.A429 without inducing any other structural perturbation. The residues R36, D40, K46, N65, T72, and E81 are all conformationally close to one another on a hydrophilic region on the NH_2-terminal domain 1. Although these residues are all located in domain 1, it is evident that there is a structural requirement for domains 1 and 2 to be intact so that cell binding can take place. The distribution of these residues on the same face of the molecule would suggest that the structure on VCAM-1 crucial

for adherence to VLA-4 is probably conformationally dependent.

The authors wish to thank Dr. Heatherbell Fong for her editorial assistance in the preparation of this manuscript.

Received for publication 30 September 1993 and in revised form 29 March 1994.

References

1. Baron, J. L., J. A. Madri, N. H. Ruddle, G. Hashim, and C. A. Janeway. 1993. Surface expression of α4 integrin by CD4 T cells is required for their entry into brain parenchyma. *J. Exp. Med.* 177:57–68.
2. Bednarczyk, J. L., J. N. Wygant, M. C. Szabo, L. Molinari-Storey, M. Renz, S. Fong, and B. W. McIntyre. 1993. Homotypic leukocyte aggregation triggered by a monoclonal antibody specific for a novel epitope expressed by the integrin β1 subunit: conversion of nonresponsive cells by transfecting human integrin α4 subunit cDNA. *J. Cell. Biochem.* 51:465–478.
3. Bernstein, F. C., T. F. Koetzle, G. J. B. Williams, E. F. Meyer, Jr., M. D. Brice, J. R. Rodgers, O. Kennard, T. Shimanouchi, and M. Tasumi. 1977. The protein databank: a computer-based archival file for macromolecular studies. *J. Mol. Biol.* 112:535–542.
4. Birdsall, H. H., C. Lane, M. N. Ramser, and C. D. Anderson. 1992. Induction of VCAM-1 and ICAM-1 on human neural cells and mechanisms of mononuclear leukocyte adherence. *J. Immunol.* 148:2717–2723.
5. Briscoe, D. M., F. J. Schoen, G. E. Rice, M. P. Bevilacqua, P. Ganz, and J. S. Pober. 1991. Induced expression of endothelial leukocyte adhesion molecules in human cardiac allografts. *Transplantation (Baltimore).* 51:537–539.
6. Carlos, T. M., B. R. Schwartz, N. L. Kovach, E. Yee, L. Osborn, G. Chi-Russo, B. Newman, R. Lobb, and J. M. Harlan. 1990. Vascular cell adhesion molecule-1 mediates lymphocyte adhesion to cytokine-activated cultured human endothelial cells. *Blood.* 76:965–970.
7. Carlos, T., N. Kovach, B. Schwartz, M. Rosa, B. Newman, E. Wayner, C. Benjamin, L. Osborn, R. Lobb, and J. Harlan. 1991. Human monocytes bind to two cytokine-induced adhesive ligands on cultured human endothelial cells: endothelial-leukocyte adhesion molecules-1 and vascular cell adhesion molecule-1. *Blood.* 77:2266–2271.
8. Chan, B. M. C., M. J. Elices, E. Murphy, and M. E. Hemler. 1992. Adhesion to vascular cell adhesion molecule 1 and fibronectin. *J. Biol. Chem.* 267:8366–8370.
9. Cybulsky, M. I., J. W. U. Fries, A. J. Williams, P. Sultan, R. Eddy, M. Byer, T. Shows, M. A. Gimbrone, and T. Collins. 1991. Gene structure, chromosome location, and basis for alternative mRNA splicing of the human VCAM1 gene. *Proc. Natl. Acad. Sci. USA.* 88:7859–7863.
10. Damle, N. K., and A. Aruffo. 1991. Vascular cell adhesion molecule 1 induces T-cell antigen receptor-dependent activation of $CD4^+$ T lymphocytes. *Proc. Natl. Acad. Sci. USA.* 88:6403–6407.
11. Eigenbrot, C., M. Randal, L. Presta, P. Carter, and A. A. Kossiakoff. 1993. X-ray structures of the antigen-binding domains from three variants of humanized anti-p185HER2 antibody 4D5 and comparison with molecular modeling. *J. Mol. Biol.* 229:969–995.
12. Elices, M. J., L. Osborn, Y. Takada, C. Crouse, S. Luhowsky, M. E. Hemler, and R. R. Lobb. 1990. VCAM-1 on activated endothelium interact with the leukocyte integrin VLA-4 at a site distinct from the VLA-4/fibronectin binding site. *Cell.* 60:577–584.
13. Ferguson, T. A., and T. S. Kupper. 1993. Antigen-independent processes in antigen-specific immunity. *J. Immunol.* 150:1172–1182.
14. Ferran, C., M. Peuchmaur, M. Desruennes, J. J. Ghoussoub, A. Cabrol, N. Brousse, C. Cabrol, J. F. Bach, and L. Chatenoud. 1993. Implications of de novo ELAM-1 and VCAM-1 expression in human cardiac allograft rejection. *Transplantation (Baltimore).* 55:605–609.
15. Gimbrone, M. A. J., M. S. Obin, A. F. Brock, E. A. Lusi, P. E. Hass, C. P. Hebert, Y. K. Yip, D. W. Leung, D. G. Lowe, W. J. Kohr, W. C. Darbonne, K. B. Bectol, and J. B. Baker. 1989. Endothelial interleukin 8: a novel inhibitor of leukocyte-endothelial interaction. *Science (Wash. DC).* 246:1601–1603.
16. Hession, C., R. Tizard, C. Vassallo, S. B. Schiffer, D. Goff, P. Moy, G. Chi-Rosso, S. Luhowskyj, R. Lobb, and L. Osborn. 1991. Cloning of an alternative form of vascular cell adhesion molecule-1 (VCAM-1). *J. Biol. Chem.* 266:6682–6685.
17. Hession, C., P. Moy, R. Tizard, P. Chisholm, C. Williams, M. Wysk, L. Burkly, K. Miyaka, P. Kincade, and R. Lobb. 1992. Cloning of murine and rat vascular cell adhesion molecule-1. *Biochem. Biophys. Res. Commun.* 183:163–169.
18. Issekutz, T. B. 1991. Inhibition of in vivo lymphocyte migration to inflammation and homing to lymphoid tissues by the TA-2 monoclonal antibody. A likely role for VLA-4 in vivo. *J. Immunol.* 147:4178–4184.
19. Jonjic, N., P. Jilek, S. Bernasconi, G. Peri, I. Martin-Padura, S. Cenzuales, E. Dejana, and A. Mantovani. 1992. Molecules involved in the adhesion and cytotoxicity of activated monocytes on endothelial cells. *J. Immunol.* 148:2080–2083.
20. Koch, A. E., J. C. Burrows, G. K. Haines, T. C. Carlos, J. M. Harlan, and S. J. Leibovich. 1991. Immunolocalization of endothelial and leukocyte adhesion molecules in human rheumatoid and osteoarthritic synovial tissues. *Lab. Invest.* 64:313–320.
21. Kunkel, T. A., J. D. Roberts, and R. A. Zakour. 1987. Rapid and efficient site-specific mutagenesis without phenotypic selection. *Methods Enzymol.* 154:367–382.
22. Miyake, K., I. L. Weissman, J. S. Greenberger, and P. W. Kincade. 1991. Evidence for a role of the integrin VLA-4 in lympho-hemopoiesis. *J. Exp. Med.* 173:599–607.
23. Miyake, K., K. Medina, K. Ishihara, M. Kimoto, R. Auerbach, and P. W. Kincade. 1991. A VCAM-like adhesion molecule on murine bone marrow stromal cells mediates binding of lymphocyte precursors in culture. *J. Cell Biol.* 114:557–565.
24. Moy, P., R. Lobb, R. Tizard, D. Olson, and C. Hession. 1993. Cloning of an inflammation-specific phosphatidyl inositol-linked form of murine vascular cell adhesion molecule-1. *J. Biol. Chem.* 268:8835–8841.
25. Norton, J., J. P. Sloane, N. Al-Saffar, and D. O. Haskard. 1992. Expression of adhesion molecules in human intestinal graft-versus-host disease. *Clin. Exp. Immunol.* 87:231–236.
26. Oppenheimer-Marks, N., L. S. Davis, D. T. Bogue, J. Ramberg, and P. Lipsky. 1991. Differential utilization of ICAM-1 and VCAM-1 during the adhesion and transendothelial migration of human T lymphocytes. *J. Immunol.* 147:2913–2921.
27. Osborn, L., C. Hession, R. Tizard, C. Vassallo, S. Luhowskyj, G. Chi-Russo, and R. Lobb. 1989. Direct expression cloning of vascular cell adhesion molecule-1, a cytokine-induced endothelial protein that binds to lymphocytes. *Cell.* 59:1203–1211.
28. Osborn, L., C. Vassallo, and C. D. Benjamin. 1992. Activated endothelium binds lymphocytes through a novel binding site in the alternately spliced domain of vascular cell cell adhesion molecule-1. *J. Exp. Med.* 176:99–107.
29. Pelletier, R. P., R. G. Ohye, A. Vanbuskirk, D. D. Sedmak, P. Kincade, R. M. Ferguson, and C. G. Orosz. 1992. Importance of endothelial VCAM-1 for inflammatory leukocytic infiltration in vivo. *J. Immunol.* 149:2473–2481.
30. Pelletier, R., R. Ohye, P. Kincade, R. Ferguson, and C. Orosz. 1993. Monoclonal antibody to anti-VCAM-1 interferes with murine cardiac allograft rejection. *Transplant. Proc.* 25:839–841.
31. Pepinsky, B., C. Hession, L. L. Chen, P. Moy, L. Burky, A. Jakubowski, E. P. Chow, C. Benjamin, G. Chi-Rosso, S. Luhowskyj, and R. Lobb. 1992. Structure/function studies on vascular cell adhesion molecule-1. *J. Biol. Chem.* 267:17820–17826.
32. Polte, T., W. Newman, and T. V. Gopal. 1990. Full length vascular cell adhesion molecule 1 (VCAM-1). *Nucleic Acids Res.* 18:5901.
33. Polte, T., W. Newman, G. Raghunathan, and T. V. Gopal. 1991. Structural and functional studies of full-length vascular cell adhesion molecule-1: Internal duplication and homology to several adhesion proteins. *DNA Cell Biol.* 10:349–357.
34. Ponder, J. W., and F. M. Richards. 1987. Tertiary template for proteins of packing criteria in the numeration of allowed sequences for different structural classes. *J. Mol. Biol.* 193:775–791.
35. Postigo, A., R. Garcia-Vicuna, F. Diaz-Gonzalez, A. G. Arroyo, M. O. De Landazuri, G. Chi-Rosso, R. Lobb, A. Laffon, and F. Sanchez-Madrid. 1992. Increased binding of synovial T lymphocytes from rheumatoid arthritis to endothelial-leukocyte adhesion molecule-1 (ELAM-1) and vascular cell adhesion molecule-1 (VCAM-1). *J. Clin. Invest.* 89:1445–1452.
36. Pulido, R., M. J. Elices, M. R. Campanero, L. Osborn, S. Schiffer, A. Garcia-Pardo, R. Lobb, M. E. Hemler, and F. Sanchez-Madrid. 1991. Functional evidence for three distinct and independently inhibitable adhesion activities mediated by the human integrin VLA-4. Correlation with distinct α4 epitopes. *J. Biol. Chem.* 266:10241–10245.
37. Rice, G. E., J. M. Munro, and M. P. Bevilacqua. 1990. Inducible cell adhesion molecule 110 (INCAM-110) is an endothelial receptor for lymphocytes. A CD11/CD18-independent adhesion mechanism. *J. Exp. Med.* 171:1369–1374.
38. Rice, G. E., J. M. Munro, C. Corless, and M. P. Bevilacqua. 1991. Vascular and non-vascular expression of INCAM-110. A target for mononuclear leukocyte adhesion in normal and inflamed human tissues. *Am. J. Pathol.* 138:385–393.
39. Rosen, G. D., J. R. Sanes, R. LaChance, J. M. Cunningham, J. Roman, and D. C. Dean. 1992. Roles for the integrin VLA-4 and its counter receptor VCAM-1 in myogenesis. *Cell.* 69:1107–1119.
40. Ruegg, C., A. A. Postigo, E. E. Sikorski, E. C. Butcher, R. Pytela, and D. J. Erle. 1992. Role of integrin $\alpha4\beta7/\alpha4\beta P$ in lymphocyte adherence to fibronectin and VCAM-1 and in homotypic cell clustering. *J. Cell Biol.* 117:179–189.
41. Ryan, D. H., B. L. Nuccie, C. N. Abboud, and J. M. Winslow. 1991. Vascular cell adhesion molecule-1 and the integrin VLA-4 mediate adhesion of human cell precursors to cultured bone marrow adherent cells. *J. Clin. Invest.* 88:995–1004.
42. Sanchez-Madrid, F., M. O. de Landazuri, G. Morago, M. Cerbrian, A.

Acevedo, and C. Bernabeu. 1986. VLA-3: a novel polypeptide association within the VLA molecular complex: cell distribution and biochemical characterization. *Eur. J. Immunol.* 16:1343–1349.
43. Seron, D., J. S. Cameron, and D. O. Haskard. 1991. Expression of VCAM-1 in normal and diseased kidney. *Nephrol. Dial. Transplant.* 6:917–922.
44. Shimuzu, Y., W. Newman, T. V. Gopal, K. J. Horgan, N. Graber, L. D. Beall, G. A. van Seventer, and S. Shaw. 1991. Four molecular pathways of T cell adhesion to endothelial cells: roles of LFA-1, VCAM-1, and ELAM-1 and changes in pathway hierarchy under different activation conditions. *J. Cell Biol.* 113:1203–1212.
45. Thornhill, M. H., S. M. Wellicome, D. L. Mahiouz, J. S. S. Lanchbury, U. Kyan-Aung, and D. O. Haskard. 1991. Tumor necrosis factor combines with IL-4 or IFN-γ to selectively enhance endothelial cell adhesiveness for T cells. The contribution of vascular cell adhesion molecule-1-dependent and -independent binding mechanisms. *J. Immunol.* 146: 592–598.
46. Unkeless, J. C., E. Scigliano, and V. H. Freeman. 1988. Structure and function of human and murine receptors for IgG. *Annu. Rev. Immunol.* 6:251–281.
47. van Dinther-Janssen, A. C. H. M., E. Horst, G. Koopman, W. Newman, R. J. Scheper, C. J. L. M. Meijer, and S. Pals. 1991. The VLA-4/VCAM-1 pathway is involved in lymphocyte adhesion to endothelium in rheumatoid synovium. *J. Immunol.* 147:4207–4210.
48. Vonderheide, R. H., and T. A. Springer. 1992. Lymphocyte adhesion through very late antigen 4: evidence for a novel binding site in the alternatively spliced domain of vascular cell adhesion molecule 1 and an additional α4 integrin counter-receptor on stimulated endothelium. *J. Exp. Med.* 175:1433–1442.
49. Watson, S. R., Y. Imai, C. Fennie, J. S. Geoffroy, S. D. Rosen, and L. A. Lasky. 1990. A homing receptor IgG chimera as a probe for adhesive ligands of lymph node high endothelial venules. *J. Cell Biol.* 110: 2221–2229.
50. Weg, V. B., T. J. Williams, R. R. Lobb, and S. Nourshargh. 1993. A monoclonal antibody recognizing vary late activation antigen-4 inhibits eosinophil accumulation in vivo. *J. Exp, Med.* 177:561–566.
51. Weiner, S. J., P. A. Kollman, D. T. Nguyen, and D. A. Case. 1986. An all atom force field for simulation of proteins and nucleic acids. *J. Comp. Chem.* 7:230–252.
52. Wuthrich, R. P. 1992. Vascular cell adhesion molecules-1 (VCAM-1) expression in murine lupus nephritis. *Kidney Int.* 42:903–914.
53. Yednock, T. A., C. Cannon, L. C. Fritz, F. Sanchez-Madrid, L. Steinman, and N. Karin. 1992. Prevention of experimental autoimmune encephalomyelitis by antibodies against $\alpha 4\beta 1$ integrin. *Nature (Lond.).* 356:63–66.